

Simulation of liquid-liquid equilibria with molecular models optimized to vapor-liquid equilibria and model development for Hydrazine and two of its derivatives

Stefan Eckelsbach¹, Thorsten Windmann¹, Ekaterina Elts¹, and Jadran Vrabec¹

1 Introduction

In the chemical industry, knowledge on fluid phase equilibria is crucial for design and optimization of many technical processes. In a chemical plant, the costs for separation facilities constitute one of the highest investment outlays, typically in the order of 40 to 80 % [PLA99]. Not only vapor-liquid equilibrium (VLE) data are of interest, e.g. for distillation columns, but also other types of phase equilibria. E.g., liquid-liquid equilibrium (LLE) data provide the basis for extraction processes.

Classically, thermodynamic data for the design of such processes have to be measured experimentally and have to be aggregated by empirical correlations. For practical applications this leads to problems. E.g., it is not possible to describe the entire fluid phase behavior consistently with a single model and set of parameters. Thus LLE data cannot be predicted reliably from VLE data (or vice versa) based on such correlations. Furthermore, the effort for measurements in the laboratory is very high, because every single fluid system of interest has to be measured individually. This approach particularly reaches its limits when multi-component fluids or systems with multiple phases are of interest due to the sheer amount of independent variables. In a recent study by Hendriks et al. [HKD+10] about the demand of thermodynamic and transport properties in the chemical industry, the urgent need for a reliable and predictive approach to describe VLE as well as LLE with a single model and parameter set is pointed out.

In this work, the capability of molecular simulation to determine fluid phase equilibria is examined, especially with respect to the problems of the classical approach described above. Molecular modeling and simulation is a modern route for the prediction of thermodynamic properties. Being based on mathematical representations of the intermolecular interactions, it has strong predictive capabilities as it

¹ Lehrstuhl für Thermodynamik und Energietechnik (ThEt), Universität Paderborn, Warburger Str. 100, 33098 Paderborn · Author to whom correspondence should be addressed: J. Vrabec. E-mail: jadran.vrabec@upb.de.

adequately covers structure, energetics and dynamics on the microscopic scale that govern the fluid behavior on the macroscopic scale. In preceding work, molecular models (force fields) were developed to accurately describe pure substance VLE data [VSH01] and were successfully assessed with respect to VLE data of binary and ternary mixtures [SVH03]. In the present work, the capability of those models to predict LLE data is studied for the binary mixture Nitrogen + Ethane. The decomposition of a randomly dispersed mixture of these two components in their LLE phases is investigated. Subsequently, the composition of the phases in equilibrium is compared to experimental data. It is shown that VLE and LLE can be predicted by molecular simulation in good agreement with experimental results.

Furthermore, three new models for Hydrazine, Monomethylhydrazine and Dimethylhydrazine were developed. They are based on quantum chemical information and were optimized to experimental data on saturated liquid density and vapor pressure. Thereafter, the models were assessed by comparing simulated VLE to experimental reference data, which they are able to reproduce.

2 Phase equilibria

2.1 Vapor-liquid equilibria

The molecular model for the mixture Nitrogen + Ethane was developed in a preceding work of our group [VHH09]. The application to mixtures can be done straightforwardly by assigning the unlike interaction parameters of the two components A and B. They are defined by the modified Lorentz-Berthelot combination rules. It was already shown in [VHH09] that one additional parameter in the equation for calculating the unlike energy parameter ϵ_{AB} , which allows to adjust the simulation results to the VLE data of the mixture, leads to an improvement of the predictive quality of the model.

$$\sigma_{AB} = \frac{\sigma_A + \sigma_B}{2} \quad (1)$$

$$\epsilon_{AB} = \xi \sqrt{\epsilon_A + \epsilon_B} \quad (2)$$

The binary parameter of the mixture Nitrogen + Ethane was defined as $\xi = 0.974$ [VHH09]. Figure 1 shows the VLE phase diagram at 200 and 290 K as determined on the basis of this mixture model in comparison to experimental data. The Peng-Robinson equation of state is given as an example of a classical correlation approach. These simulations coincide closely with the experimental reference values for pressures below 7 MPa. With raising pressure, the deviations also increase, but the values are closer to the experiment than the Peng-Robinson equation of state, which overestimates the critical region and shows significant deviations particularly on the saturated liquid line.

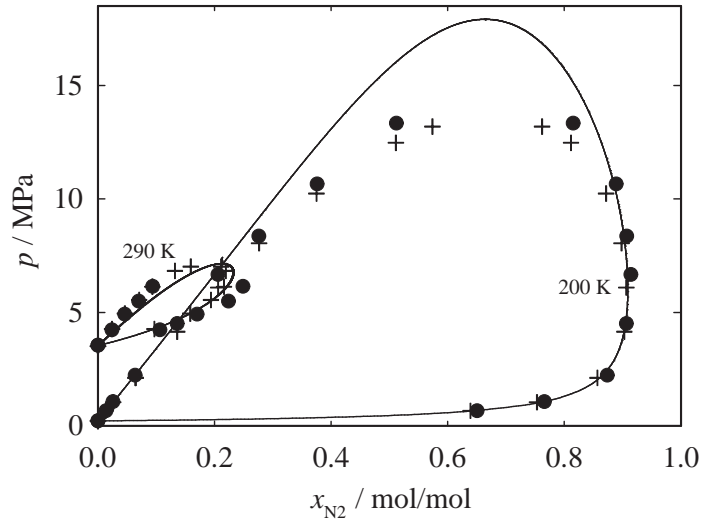


Fig. 1 Vapor-liquid equilibria of the mixture Nitrogen and Ethane: simulation results (●); experimental data (+) [DDB10]; Peng-Robinson equation of state (—). The statistical uncertainties of the present data are within symbol size.

2.2 Liquid-liquid equilibria

Molecular dynamics simulations were performed for a mixture of 20 000 molecules, consisting of 40 mol-% Ethane and 60 mol-% Nitrogen. The two components were randomly dispersed in the initial configuration. The simulations were carried out with our molecular dynamics code *ls1 mardyn*. They were performed in a canonical ensemble and the length of one time step was set to 2 fs.

Starting from a randomly dispersed mixture, it was found that the system decomposes spontaneously into two coexisting liquid phases. As an example, the progress of a simulation at the pressure 11.03 MPa and the temperature 128 K is plotted in figure 2. The simulation required about $2.4 \cdot 10^7$ time steps to lead to an equilibrated state, which represents a typical duration of the present simulations of around 50 ns. Thereafter, the two phases can be clearly identified by the mole fraction over the length of the simulation volume, which is presented in figure 3. This provides the ability of predicting the LLE phase behavior for different thermodynamic conditions. The comparison of the present results with experimental data is shown in figure 4. The simulated mole fractions agree well with the experimental data and so they also reproduce the pressure dependence of the LLE.

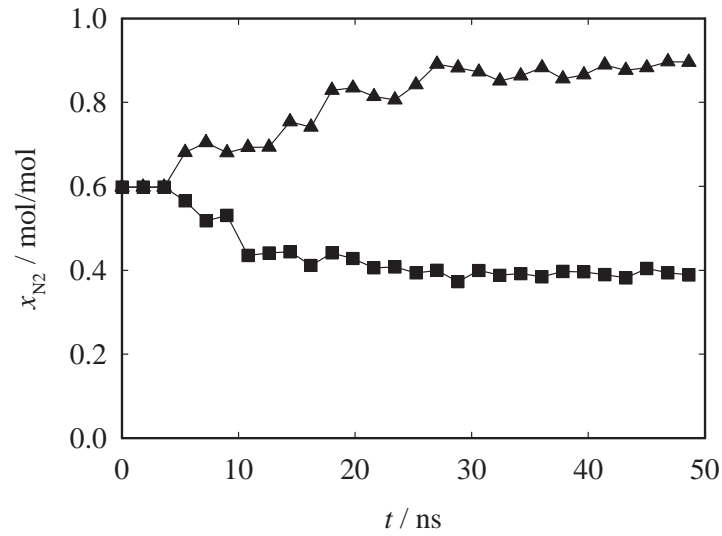


Fig. 2 Progress of the mole fraction of Nitrogen in phase 1 (▲) and phase 2 (■) over the duration of the simulation t : The simulation was performed for a temperature of 128 K and a pressure of 11.03 MPa.

3 Hydrazines

3.1 Molecular model class

The present molecular models include three groups of parameters. These are (1) the geometric parameters, specifying the positions of different interaction sites, (2) the electrostatic parameters, defining the polar interactions in terms of point charges, dipoles or quadrupoles, and (3) the dispersive and repulsive parameters, determining the attraction by London forces and the repulsion by electronic orbital overlaps. Here, the Lennard-Jones (LJ) 12-6 potential [Jon24, Jon24a] was used to describe the dispersive and repulsive interactions. The total intermolecular interaction energy thus writes as

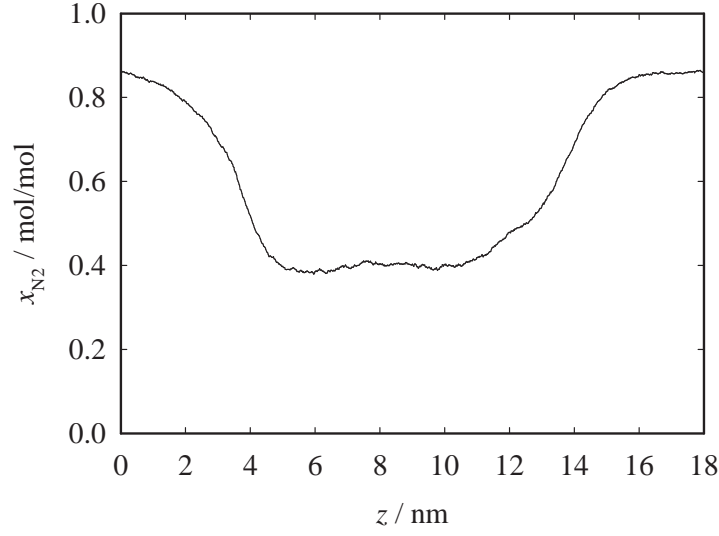


Fig. 3 Mole fraction of Nitrogen over the length of the simulation volume in z direction: The simulation was carried out at a temperature of 128 K and a pressure of 11.03 MPa.

$$\begin{aligned}
 U = & \sum_{i=1}^{N-1} \sum_{j=i+1}^N \left\{ \sum_{a=1}^{S_i^{\text{LJ}}} \sum_{b=1}^{S_j^{\text{LJ}}} 4\epsilon_{ijab} \left[\left(\frac{\sigma_{ijab}}{r_{ijab}} \right)^{12} - \left(\frac{\sigma_{ijab}}{r_{ijab}} \right)^6 \right] + \right. \\
 & \sum_{c=1}^{S_i^e} \sum_{d=1}^{S_j^e} \frac{1}{4\pi\epsilon_0} \left[\frac{q_{ic}q_{jd}}{r_{ijcd}} + \frac{q_{ic}\mu_{jd} + \mu_{ic}q_{jd}}{r_{ijcd}^2} \cdot f_1(\mathbf{\omega}_i, \mathbf{\omega}_j) + \frac{q_{ic}Q_{jd} + Q_{ic}q_{jd}}{r_{ijcd}^3} \cdot f_2(\mathbf{\omega}_i, \mathbf{\omega}_j) + \right. \\
 & \left. \left. \frac{\mu_{ic}\mu_{jd}}{r_{ijcd}^3} \cdot f_3(\mathbf{\omega}_i, \mathbf{\omega}_j) + \frac{\mu_{ic}Q_{jd} + Q_{ic}\mu_{jd}}{r_{ijcd}^4} \cdot f_4(\mathbf{\omega}_i, \mathbf{\omega}_j) + \frac{Q_{ic}Q_{jd}}{r_{ijcd}^5} \cdot f_5(\mathbf{\omega}_i, \mathbf{\omega}_j) \right] \right\}, \quad (3)
 \end{aligned}$$

where r_{ijab} , ϵ_{ijab} , σ_{ijab} are the distance, the LJ energy parameter and the LJ size parameter, respectively, for the pair-wise interaction between LJ site a on molecule i and LJ site b on molecule j . The permittivity of the vacuum is ϵ_0 , whereas q_{ic} , μ_{ic} and Q_{ic} denote the point charge magnitude, the dipole moment and the quadrupole moment of the electrostatic interaction site c on molecule i and so forth. The expressions $f_x(\mathbf{\omega}_i, \mathbf{\omega}_j)$ stand for the dependence of the electrostatic interactions on the orientations $\mathbf{\omega}_i$ and $\mathbf{\omega}_j$ of the molecules i and j , cf. [AT87, GG84]. Finally, the summation limits N , S_x^{LJ} and S_x^e denote the number of molecules, the number of LJ sites and the number of electrostatic sites, respectively.

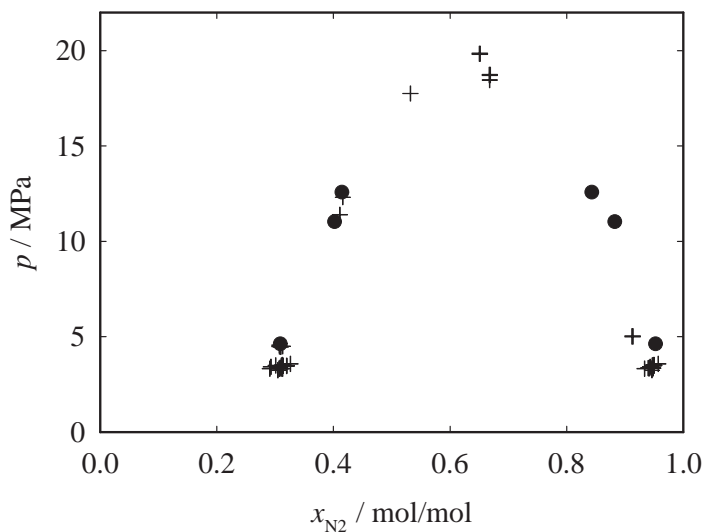


Fig. 4 Liquid-liquid equilibria of the mixture Nitrogen + Ethane: simulation results (●) for a temperature of approximately 128 K; experimental data (+) for a temperature of 126.7 K to 129 K [DDB10].

3.2 Molecular pure substance models

For all molecular models developed in the present work, the internal degrees of freedom were neglected and the models were chosen to be rigid. As a first step, the geometric data of the molecules, i.e. bond lengths, angles and dihedrals, were determined by QC calculations. Therefore, a geometry optimization was performed via an energy minimization using the GAMESS (US) package [SBB+93]. The Hartree-Fock level of theory was applied with a relatively small (6-31G) basis set. All LJ parameters and the charge magnitudes were initially taken from prior models and fine tuned during the model parameter optimization to vapor pressure and saturated liquid density.

Figure 5 shows the developed molecular models.

The results for saturated densities obtained with the present model are compared to the available experimental data [GGM09, DDB10, DIP06] and to the simulation results by Gutowski *et al.* [GGM09] in figure 6.

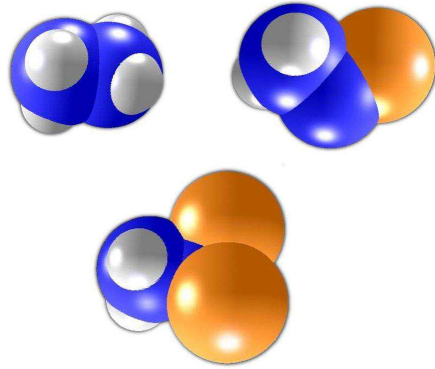


Fig. 5 Snapshot of Hydrazine (top, left), Monomethylhydrazine (top, right) and Dimethylhydrazine.

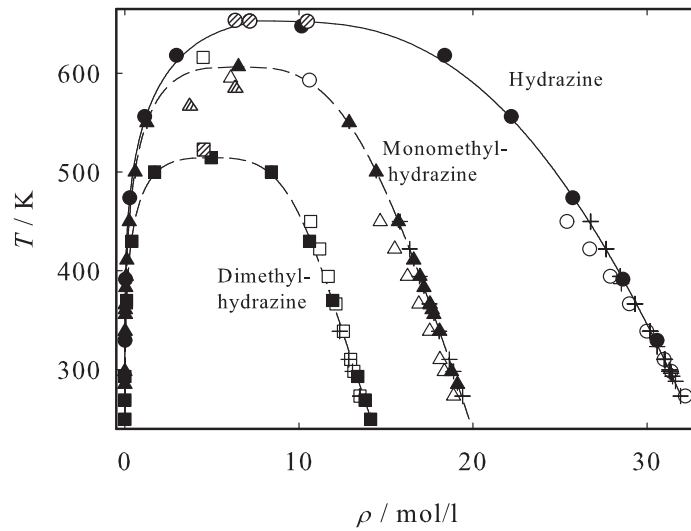


Fig. 6 Saturated densities of Hydrazine (●), Monomethylhydrazine (▲) and Dimethylhydrazine (■); (striped symbols) experimental critical data [GGM09, DDB10, DIP06, MDB10]; (+) experimental saturated liquid densities [DDB10, DIP06]; (full symbols) simulation data on the basis of the present models; (empty symbols) simulation data (saturated liquid only) by Gutowski et al. [GGM09]; (—) correlation of experimental data [DIP06]; (- - -) correlation of present simulation data [Gug45]. The statistical uncertainties of the present data are within symbol size.

3.3 Binary vapor-liquid equilibria

Based on the discussed three molecular hydrazine models, VLE data were predicted for all three binary Hydrazine mixtures with Water as well as for the mixture Dimethylhydrazine + Hydrazine.

3.3.1 Water + Hydrazine

Figure 7 shows the isobaric VLE of Water + Hydrazine at 0.1013 MPa from experiment [DDB10, LD02, UOY50], simulation and Peng-Robinson EOS. The mixture is azeotropic, having a temperature maximum. The azeotropic point is at $x_{\text{H}_2\text{O}} \approx 0.41$ mol/mol. The experimental vapor pressure by Uchida *et al.* [UOY50] at 388.25 K and $x_{\text{H}_2\text{O}} = 0.6925$ mol/mol was taken to adjust the binary parameter of the molecular model ($\xi = 1.3$). Considering the substantial experimental uncertainties, both data sets agree very favorably.

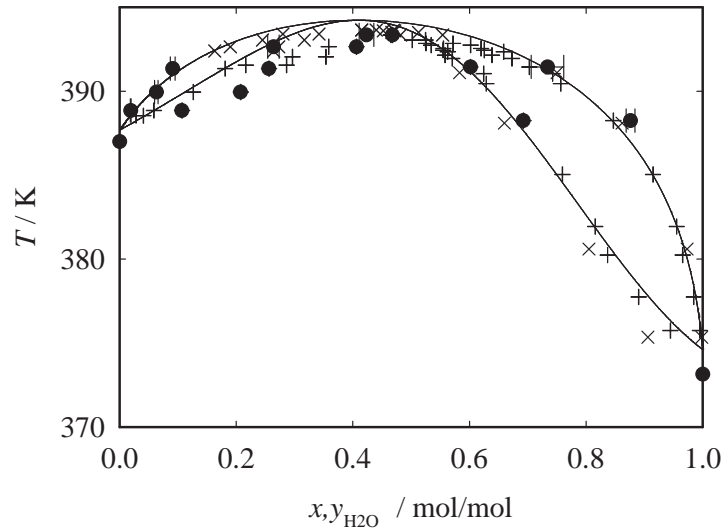


Fig. 7 Isobaric vapor-liquid phase diagram of Water + Hydrazine at 0.1013 MPa: (×) experimental data by Lobry de Bruyn and Dito [LD02]; (+) experimental data by Uchida *et al.* [UOY50]; (●) present simulation data with $\xi=1.3$; (—) Peng-Robinson EOS with $k_{ij}=-0.1325$.

3.3.2 Monomethylhydrazine + Water

Figure 8 depicts the VLE of Monomethylhydrazine + Water at ambient pressure. Like aqueous Hydrazine, this mixture is azeotropic, having a temperature maximum. In this case, the azeotropic point lies at $x_{\text{CH}_3-\text{N}_2\text{H}_3} \approx 0.25$ mol/mol. The experimental data by Ferriol *et al.* [FLC+92] at 372.55 K and $x_{\text{CH}_3-\text{N}_2\text{H}_3} = 0.476$ mol/mol were taken to adjust the binary parameter of the molecular model ($\xi = 1.3$). In the Water-rich region, to the left of the azeotropic point in figure 8, VLE simulations were not feasible, because of sampling problems. Considering the substantial experimental uncertainties, the data sets from all three approaches agree very favorably.

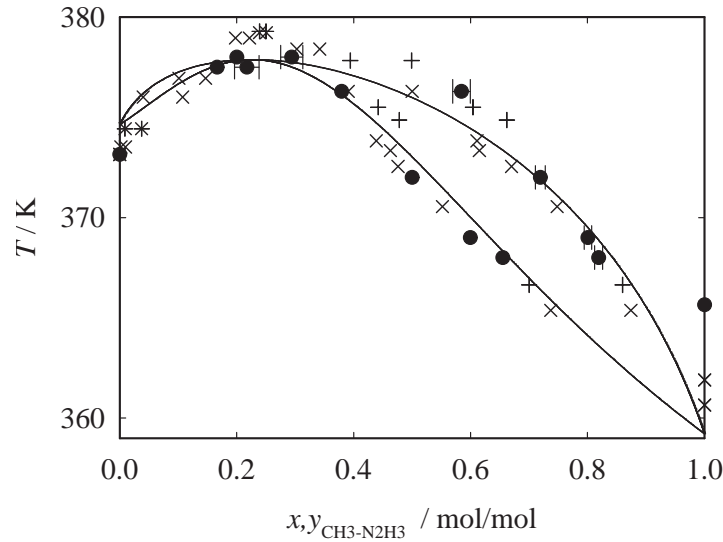


Fig. 8 Isobaric vapor-liquid phase diagram of Monomethylhydrazine + Water at 0.1013 MPa: (×) experimental data by Ferriol et al. [FLC+92]; (+) experimental data by Cohen-Adad et al. [CAG87]; (●) present simulation data with $\xi=1.3$; (—) Peng-Robinson EOS with $k_{ij}=-0.197$.

3.3.3 Dimethylhydrazine + Water

Figure 9 shows the isobaric VLE of Dimethylhydrazine + Water at 0.1013 MPa from experiment, simulation and the Peng-Robinson equation of state. In contrast to the the previous two binary systems, this mixture is zeotropic. The experimental vapor pressure by Ferriol et al. [FLC+92] at 345.17 K and $x_{(\text{CH}_3)_2-\text{N}_2\text{H}_2} = 0.571$ mol/mol was taken to adjust the binary parameter of the molecular model ($\xi = 1.3$). It can be seen in the figure 9 that the results obtained by molecular simulation agree well with the experimental results on the saturated liquid line, but overestimate the Dimethylhydrazine content on the saturated vapor line for intermediate compositions.

3.3.4 Dimethylhydrazine + Hydrazine

The VLE of Dimethylhydrazine + Hydrazine is presented in figure 10 at ambient pressure. This system is zeotropic. The experimental vapor pressure by Pannetier and Mignotte [PM61] at 346.35 K and $x_{(\text{CH}_3)_2-\text{N}_2\text{H}_2} = 0.4717$ mol/mol was taken to adjust the binary parameter of the molecular model ($\xi = 1.01$). It can be seen that simulation results match almost perfectly with the experimental data on the saturated liquid line. On the saturated vapor line, the experimental data and the simulation results exhibit some scatter, but the agreement is reasonable.

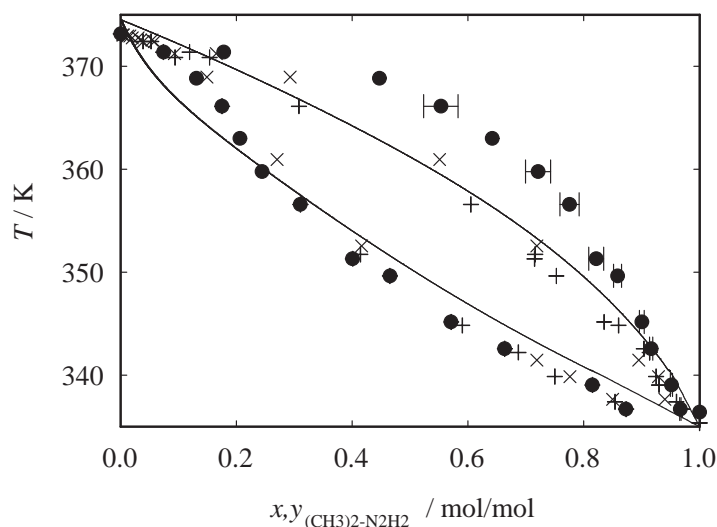


Fig. 9 Isobaric vapor-liquid phase diagram of Dimethylhydrazine + Water at 0.1013 MPa: (×) experimental data by Carleton [Car56]; (+) experimental data by Ferriol *et al.* [FLC+92]; (●) present simulation data with $\xi=1.3$; (—) Peng-Robinson EOS with $k_{ij}=-0.285$.

4 Conclusion

It was shown that molecular models that were adjusted to VLE data provide the option to simulate LLE and predict their pressure dependence. The simulations yield reliable data that are in good agreement with experimental values. In contrast to the classical approach to provide phase equilibrium data, this route has the capability of predicting VLE and LLE data with a single model and set of parameters.

Furthermore, molecular modeling and simulation was applied to predict the VLE phase behavior of pure fluids and binary mixtures containing Hydrazine and two of its derivatives. New molecular models were developed for Hydrazine, Monomethylhydrazine and Dimethylhydrazine, partly based on quantum chemical information on molecular geometry and electrostatics. Experimental data on the saturated liquid density and the vapor pressure were taken into account to optimize the pure substance models. These pure substance properties were represented accurately from the triple point to the critical point.

For an optimized description of the binary VLE, the unlike dispersive interaction was adjusted for all studied binary systems to a single experimental vapor pressure of the mixture in the vicinity of ambient conditions. With these binary mixture models, VLE data were predicted for a temperature and composition range. The predictions show a good agreement with experimental binary VLE data that were not considered in the model development.

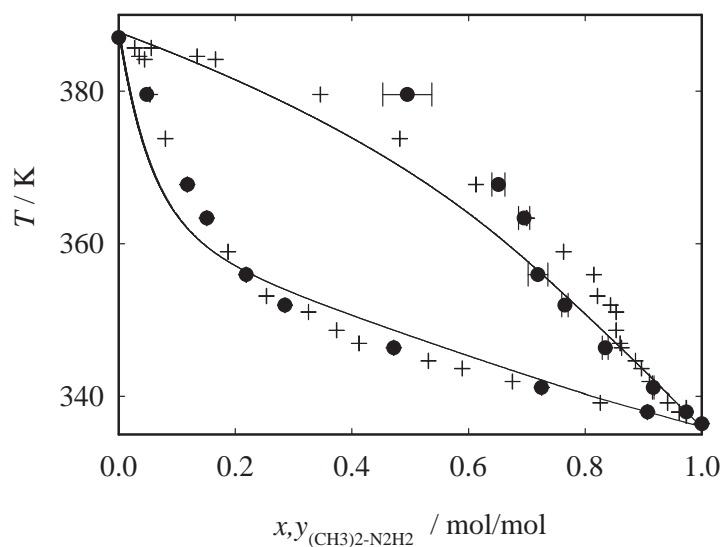


Fig. 10 Isobaric vapor-liquid phase diagram of Dimethylhydrazine + Hydrazine at 0.1013 MPa: (+) experimental data by Pannetier and Mignotte [PM61]; (●) present simulation data with $\xi=1.01$; (—) Peng-Robinson EOS with $k_{ij}=-0.1$.

In this work, molecular modeling and simulation was used to predict the VLE phase behavior and the thermodynamic properties of pure hydrazines and binary aqueous hydrazine mixtures, for which experimental data were available for comparison. The presented molecular models were able to well reproduce the experimental data that were not considered in the model development. Thus, these new models could also be valuable for the prediction of properties under different conditions and for systems, where no experimental data are available.

5 Acknowledgements

We gratefully acknowledge support by Deutsche Forschungsgemeinschaft. This work was carried out under the auspices of the Boltzmann-Zuse Society (BZS) of Computational Molecular Engineering. The simulations were performed on the NEC SX-9, the NEC Nehalem Cluster and the Cray XE6 (Hermit) at the High Performance Computing Center Stuttgart (HLRS).

References

- [AT87] Allen, M. P.; Tildesley, D. J.: Computer simulations of liquids. *Oxford University Press, Oxford* **1987**.
- [CAG87] Cohen-Adad, M. T.; Allali, I.; Getzen F. W. *J. Solution Chem.* **1987** *16*, 659.
- [Car56] Carleton, L. T. *Ind. Eng. Chem. Chem. Eng. Data Series* **1956** *1*, 21.
- [DDB10] Dortmund Datenbank, Mixture Properties. Version 6.3.0.384 **2010**.
- [DIP06] Rowley, R. L.; Wilding, W. V.; Oscarson, J. L.; Yang, Y.; Zundel, N. A.; Daubert, T. E.; Danner, R. P.: DIPPR Data Compilation of Pure Chemical Properties. *Design Institute for Physical Properties, AIChE, New York* **2011**.
- [FLC+92] Ferriol, M.; Laachach, A.; Cohen-Adad, M. T.; Getzen, F. W.; Jorat, L.; Noyel, G.; Huck, J.; Bureau, J. C. *Fluid Phase Equilibr.* **1992** *71*, 287.
- [GG84] Gray, C. G.; Gubbins K. E.: Theory of molecular fluids, 1. Fundamentals. *Clarendon Press, Oxford* **1984**.
- [GGM09] Gutowski, K. E.; Gurkan, B.; Maginn E. J. *Pure Appl. Chem.* **2009** *81*, 1799.
- [Gug45] Guggenheim, E. A. *J. Chem. Phys.* **1945** *13*, 253.
- [HKD+10] Hendriks, E.; Kontogeorgis, G. M.; Dohrn, R.; de Hemptinne, J. C.; Economou I. G.; Žilnik, L. F.; Vesovic, V. *Ind. Eng. Chem. Res.* **2010** *49*, 11131.
- [Jon24] Jones, J. E. *Proc. Roy. Soc.* **1924** *106A*, 441.
- [Jon24a] Jones, J. E. *Proc. Roy. Soc.* **1924** *106A*, 463.
- [LD02] Lobry de Bruyn, C. A.; Dito, J. W. *Proc. Sec. Sci./K. Akad. Wet. Amsterdam* **1902-1903** *5*, 171.
- [MDB10] Hradetzky, G.; Lempe, D. A.: Merseburg Data Bank MDB for thermophysical data of pure compounds. Revision 7.1.0 **2010**.
- [PLA99] Prausnitz, J. M.; Lichtenthaler, R. N.; de Azevedo, E. G.: Molecular Thermodynamics of Fluid-Phase Equilibria. *Prentice-Hall: Upper Saddle River, New Jersey* **1999**.
- [PM61] Pannetier, G.; Mignotte, P. *Bull. Soc. Chim. Fr.* **1961** *143*, 985.
- [SBB+93] Schmidt, M. W.; Baldrige, K. K.; Boatz, J. A.; Elbert, S. T.; Gordon, M. S.; Jensen, J. H.; Koseki, S.; Matsunaga, N.; Nguyen, K. A.; Shujun, S; Windus, T. L.; Dupuis, M.; Montgomery, A. M. *J. Comput. Chem.* **1993** *14*, 1347.
- [SVH03] Stoll, J.; Vrabec, J.; Hasse, H. *AIChE J.* **2003** *49*, 2187.
- [UOY50] Uchida, S.; Ogawa, S.; Yamaguchi, M. *Jap. Sci. Rev. Eng. Sci.* **1950** *1*, 41.
- [VHH09] Vrabec, J.; Huang, Y.-L.; Hasse, H. *Fluid Phase Equilibr.* **2009** *279*, 120.
- [VSH01] Vrabec, J.; Stoll, J.; Hasse, H. *J. Phys. Chem. B* **2001** *105*, 12126.